Effect of Mg based addition to Upgraded Brown Coal on the Ash Deposition Behavior During Combustion

Katsuya Akiyama[a], Haeyang Pak[a], Yasuaki Ueki[b], Ryo Yoshiie[c], Ichiro Naruse[c]

E-mail address: akiyama.katsuya@kobelco.com (K.Akiyama)
[a] Mechanical Engineering Research Laboratory, KOBE STEEL, LTD., 1-5-5 Takatsukadai, Nishi-ku, Kobe, 651-2271, JAPAN
[b] Energy Science Division, EcoTopia Science Institute, NAGOYA UNIVERSITY, Furo-cho, Chikusa-ku, Nagoya, 464-8603, JAPAN
[c] Department of Mechanical Science & Engineering, NAGOYA UNIVERSITY, Furo-cho, Chikusa-ku, Nagoya, 464-8603, JAPAN

Abstract

The objectives of this study are to evaluate the effect of MgO addition with the coal on the reduction of ash deposition during upgraded brown coal (UBC) combustion and to understand the reduction mechanisms of ash deposition. The melting temperature of the UBC ash is 1494 K, which is relatively lower than that of bituminous coal ash. Before the actual ash deposition experiments, the molten slag fraction in the UBC ash was estimated by means of chemical equilibrium calculations while varying the mixing mass ratio of MgO to coal ash. The results of a simulation indicate that the MgO addition played a role in decreasing in molten slag fraction. It was confirmed that Mg formed solid composites with Si, Fe, Al, Ca, and Mn and played a role in decreasing the molten slag fraction in ash on the tube. As a next step, ash deposition tests were conducted using a pilot-scale pulverized coal combustion furnace equipped with a refractory wall. As a result, the MgO addition contributed to the decreasing rate of ash deposition even for the UBC. The smaller the particle diameter of MgO additive is, the more the rate of ash deposition lowers. These calculations and experimental results suggested that one of the reduction mechanisms was due to the production of solid phase compositions of alumino-silicates due to MgO addition.

Key Words: Reduction of ash deposition, MgO additive, Upgraded brown coal (UBC)

1. Introduction

Bituminous coals, which are categorized as high-rank coals, are most commonly consumed in industrial sectors. In contrast, demand for low-rank coals, such as sub-bituminous coal, lignite, and brown coal, is limited because of its lower calorific value and/or higher moisture content. Therefore, low-rank coal is usually utilized as fuel only in some specific local regions around its mines. Recently, there have been demands for a technology to utilize the low-rank coals as a common fuel because of the limited availability of reserves of the high-rank coals. As some Indonesian low-rank coals have high moisture contents, their heating values are relatively low. However, the contents of the ash, nitrogen, and sulfur in these coals are smaller. If the effective drying or dewatering technologies for these coals could be developed, it would be possible to use them as new fossil fuels. Kobe Steel has developed an UBC process based on the slurry dewatering process [1-3]. Akiyama *et al.* also evaluated the combustion characteristics of UBC [4]. However, the ash melting points of Indonesian low-rank coals are relatively low. Therefore, slagging and fouling problems may occur in pulverized coal

combustion boilers. The ash deposits on the heat exchanger tubes reduce the overall heat transfer coefficient because of its low thermal conductivity. Consequently, it is difficult to use such low-rank coals alone in the pulverized coal combustion boiler.

Ash deposition phenomena are influenced by coal type (ash compositions, melting temperature, and distribution of mineral matter), reaction atmosphere, particle temperature, the surface temperature of heat exchanger tubes and tube materials, flow dynamics, and so forth. Several reviews relating to the ash deposition characteristics have already been reported [5]. For instance, Raask elucidated the deposit initiation [6], and Walsh *et al.* [7] and Baxter [8] studied the deposition characteristics and growth. Beer *et al.* [9] attempted to develop theories of ash behavior. Benson *et al.* [10] summarized the behavior of ash formation and deposition during coal combustion. Naruse *et al.* [11] evaluated the ash deposition characteristics under high-temperature conditions. Vuthaluru *et al.* [12] evaluated the ash formation of brown coal. Li *et al.* [13] investigated coal char-slag transition under oxidation conditions. Bai *et al.* [14] studied the characterization of low-temperature coal ash at high temperatures under a reducing atmosphere. Abbott *et al.* [15] investigated the adhesion force between slag and oxidized steel. Harb *et al.* [16] predicted ash behavior using a chemical equilibrium calculation. Hansen *et al.* [17] quantified ash fusibility using differential scanning calorimetry, and Ichikawa *et al.* [18] measured the liquid phase ratio of ash using differential thermal analysis. Song *et al.* [19] investigated the effect of coal ash composition on ash fusion temperatures. Even for those references, however, precise and quantitative knowledge of the deposition of coal ash with a low-melting temperature during coal combustion has been insufficient. Our previous studies [20] have proven that the molten slag fraction in ash obtained by chemical equilibrium calculations is one useful index with which to predict the coal blending method to reduce the deposition fraction of ash. First, the influence that each ash constituent affected the molten slag fraction is evaluated. As a result, It has been understood that the MgO was most effective to control the molten slag fraction of ash. Several papers relating to the Mg based fuel additive for the boiler have already been reported. Pohl et al. [21] invested the effect the injection of $Mg(OH)_2$ slurry on the reduction of the slagging in the coal fired boiler. Libutti et al. [22] and Williams et al. [23], Sinha [24] studied the effect the injection of MgO additive on the reduction of fire side corrosion in the oil fired boiler. Even for those references, however, the mechanisms that MgO addition into the coal affect the reduction of ash deposition has not been elucidated.

The objectives of this study are to evaluate the effect of MgO addition into the coal on the reduction of ash deposition for UBC and to understand the reduction mechanisms of ash deposition. The melting temperature of the UBC ash is 1494 K, which is relatively lower than that of bituminous coal ash. Before the actual ash deposition experiments, the molten slag fraction in the UBC ash was estimated by means of chemical equilibrium calculations while changing the mixing mass ratio of MgO to coal ash. As the next step, ash deposition tests were also conducted using a pilot-scale pulverized coal combustion furnace equipped with a refractory wall.

2. UBC Process

Figure 1 shows a schematic diagram of the UBC process. The UBC process developed by Kobe Steel can increase the quality of low-rank coal by means of a slurry dewatering technique at a low temperature and pressure without chemical reactions. Kobe steel started developing this UBC process for Australian brown coal in 1993. The 3 t/d pilot plant for Indonesian UBC has been operated successfully since 2001. Recently, the 600 t/d demonstration plant has been operated in Satui, South Kalimantan. In the UBC process, the low-rank coal is first crushed and then is mixed with oil and a small amount of asphalt to produce the slurry. This coal–oil slurry is heated in order to be dewatered. The UBC produced

adsorbs very little moisture since the asphalt can deactivate the active sites effectively. After the coal is separated from the oil, it is dried and pressed to make transportable briquettes. As mentioned above, the UBC process can effectively remove the moisture in low-rank coal and can increase its heating value without changing its other properties. Therefore, the UBC produced from Indonesian low-rank coal has useful properties, such as low nitrogen, sulfur, and ash contents. However, this process cannot change the melting point of UBC ash any more.

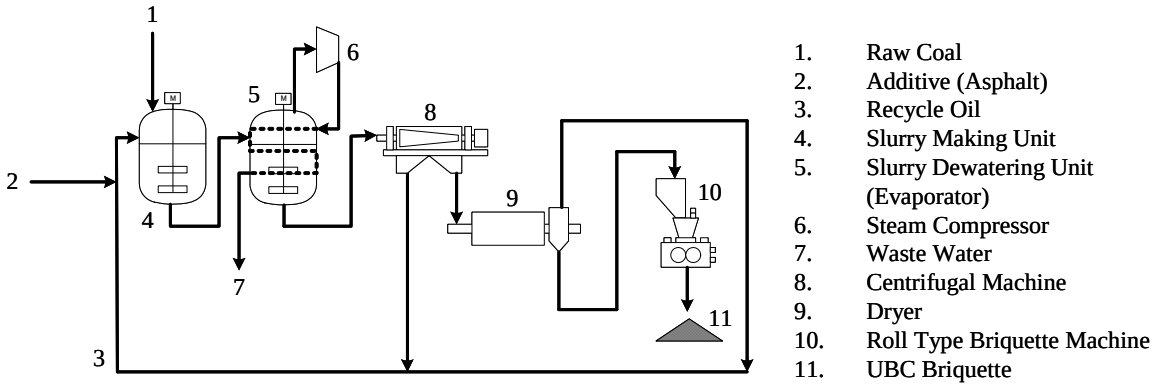

Figure 1. Schematic diagram of UBC process.

3. Method of Chemical Equilibrium Calculations

We used the Indonesian UBC and bituminous coal with different melting temperatures and ash compositions, as shown in Table 1. As seen from the table, the initial deformation temperature of UBC E under the oxidizing condition is lower than that of Coal A3. For the ash in the UBC E, Fe_2O_3 content was larger than that of Coal A3. The ash particles tend to adhere more on the tube as the amount of molten particles increases [20]. In this calculation, therefore, we calculated the molten fraction of each ash by chemical equilibrium theory, using Fact Sage Ver. 6.1 software [25-26]. The Fact Sage software, which was used for the chemical equilibrium calculations in this paper, can simulate compositions of non-ideal liquid species in terms of the minimization of Gibbs's free energy of all phases as functions of temperature and compositions since this software has special thermodynamic databases on non-ideal liquid species. Table 2 shows the conditions of the chemical equilibrium calculations. The gaseous compositions given were assumed to be near a burner in the pulverized coal combustion boiler. The ash deposition area is always exposed to the reducing gas. Therefore, the partial pressures of CO, CO_2, and H_2 gas were fixed in the calculations. We performed these calculations in 50 K increments to determine the mass percentage of molten slag in the ash in the temperature range 1273–2073 K.

4. Experimental Section

Figure 2 shows a schematic diagram of the pilot-scale pulverized coal combustion refractory furnace used in this study. The furnace was 3.65 m long and 0.4 m in inner diameter. It was insulated by a refractory material to reduce the heat loss. The pulverized coal weighed by the volumetric feeder was transported to the burner with nitrogen gas. The primary air at ambient temperature and the secondary air heated at 573 K were supplied separately. City gas was supplied to the furnace in order to heat it to 1750 K. In the experiments, we inserted a thermocouple and a gas sampling probe into the furnace to measure the gas temperature and gaseous concentrations, respectively. The coal was pulverized with 85% in mass fraction less than 75 μm.

Table 1. Properties of coals tested.

Coal sample			UBC E	Coal A3
Heating value [MJ/kg]			25.27	29.02
Proximate analysis [wt%, dry]	Ash		6.27	12.18
	Volatile matter		49.09	32.83
	Fixed carbon		44.64	54.99
Fuel ratio [-]			0.91	1.67
Ultimate analysis [wt%, d.a.f]	Carbon		72.91	81.39
	Hydrogen		5.65	5.26
	Nitrogen		1.05	1.83
	Sulfur		0.34	0.50
	Oxygen (Balance)		20.05	11.02
Ash fusion temperature [K]	Oxidizing	Initial deformation	1440	1753
		Hemisperical	1494	>1823
		Fluid	1651	>1823
	Reducing	Initial deformation	1433	1607
		Hemisperical	1453	1821
		Fluid	1473	>1823
Ash compositions [wt%]	SiO_2		41.10	65.90
	Al_2O_3		12.50	22.90
	CaO		10.30	1.08
	Fe_2O_3		16.30	4.58
	MgO		8.36	0.79
	Na_2O		0.13	0.47
	K_2O		1.50	1.37
	SO_3		8.34	0.62
	P_2O_5		0.04	0.31
	TiO_2		0.64	1.37
	V_2O_5		0.03	0.07
	MnO		0.26	0.03

Table 2. Conditions of the chemical equilibrium calculations.

Temperature (K)		1273 ~ 2073
Gas composition (%)	O_2	8.3×10^{-8}
	CO_2	12.3
	CO	8.2
	H_2	1.5
	N_2	70.6
	H_2O	7.4
Ash composition (wt%)	SiO_2, Al_2O_3, CaO, Fe_2O_3, MgO, Na_2O, K_2O, SO_3 P_2O_5, TiO_2, V_2O_5, MnO	

We used MgO with a mean particle diameter of 0.2 μm and 5 μm as the additive to the UBC. The purity of each additive is 99.9%. The pulverized UBC and MgO additive were mixed using a mixer before the ash deposition test. Table 3 shows the experimental conditions. The heat load was fixed at a given value of 149 kW for all the tests. The oxygen concentration of the flue gas at the furnace outlet was fixed at a given value of 1.0% as a dry basis. The oxygen concentration at the inserted ash deposition tube was approximately 1.5% as a dry basis. We inserted the deposition probe, made of stainless steel (SUS304), 1.9 m from the burner tile where the temperature was about 1573 K. The temperature around the ash deposition tube is similar to that in the slagging area near the burner in the pulverized coal combustion boiler. The length and outer diameter of the ash deposition tube were 0.2 and 0.0318 m, respectively. The deposition probe mainly consisted of a test piece for deposition and a water-cooled probe.

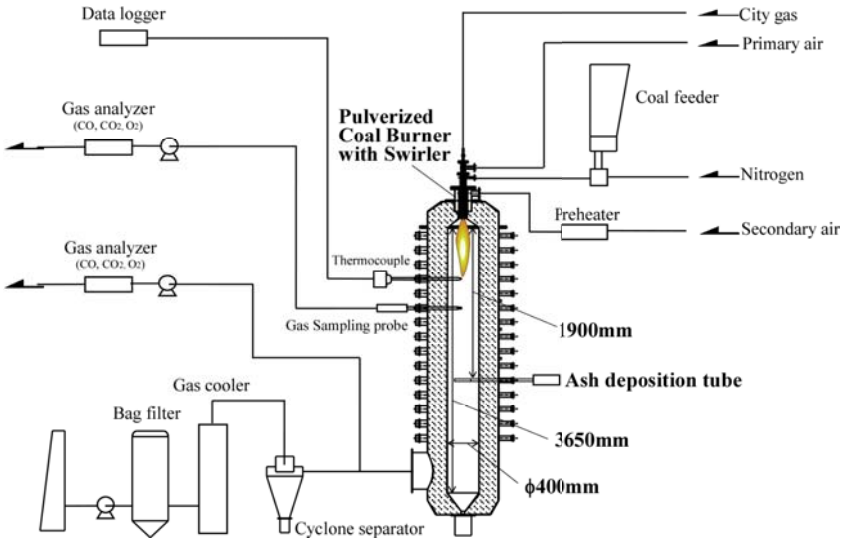

Figure 2. Schematic diagram of a pilot-scale pulverized coal combustion refractory furnace.

Table 3. Experimental conditions,

Coal sample	UBC E
Heating Value [kW]	149
Combustion stoichiometric ratio [-]	1.05
Oxygeon concentration at furnace outlet [%]	1.0
Oxygeon concentration around ash deposition tube [%]	1.5
Gas and mean particle temperature around ash deposition tube [K]	1573
Gas velocity at 1573 K [m/s]	~2.6
Surface temperature of ash deposition tube [K]	773
Ash deposition tube diameter [mm]	31.8
Ash deposition tube length [mm]	200
Exposure time for ash deposition [min]	100
Mean particle diameter of MgO [μm]	0.2, 5
Additive fraction of MgO to UBC ash [wt%]	0, 25, 50

Two thermocouples were installed between the test piece and the water-cooled probe. We assumed the temperatures measured by those thermocouples to be the surface temperature of the test piece of deposition. The surface temperature was controlled at 773 K by adjusting the flow rate of cooling water inside the tube. We observed the cross-sectional structures and compositions of ash particles before adhering to the tube and the deposition layer on the tube using scanning electron microscopy (SEM) and electron probe micro analysis (EPMA). The ash particles just before adhering to the tube were also collected in the filter, using a water cooled sampling probe and a suction pump.

5. Results and discussion

5.1. Fraction of the molten slag with and without MgO addition obtained by chemical equilibrium calculations

Figure 3 shows the calculated results of the molten slag fraction in ash for two types of coal ash. The molten slag fraction is defined as the content of molten slag in the total ash. For UBC E ash, the molten slag formed at relatively low temperatures. For Coal A3 ash, however, the molten slag did not form at temperature less than 1273 K.

Figure 4 shows the relationship between the additive fraction of each ash component in UBC E ash and the increase-decrease mass ratio of the molten slag at 1573 K. In the

calculations, we simply added each ash component to the UBC E ash sample. The increase-decrease mass ratio of molten slag is defined as the mass ratio of the molten slag with additive of each ash component to the molten slag without additive. Therefore, a ratio of less than 1 means that production of the molten slag actually decreased even if an additive was added to the ash. This figure shows that the MgO addition was the most effective for the reduction of the increase-decrease mass ratio of molten slag fraction of the UBC E ash. Under a condition of 25 wt% addition of MgO, production of molten slag in UBC E ash almost halved.

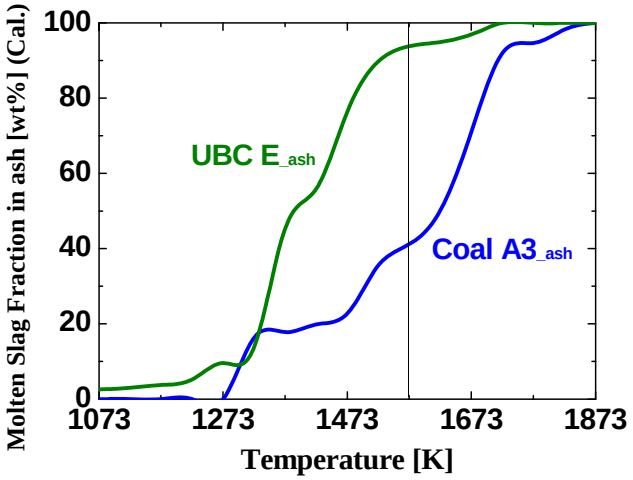

Figure 3. Calculated results of the molten slag fraction in ash for four types of coal ash.

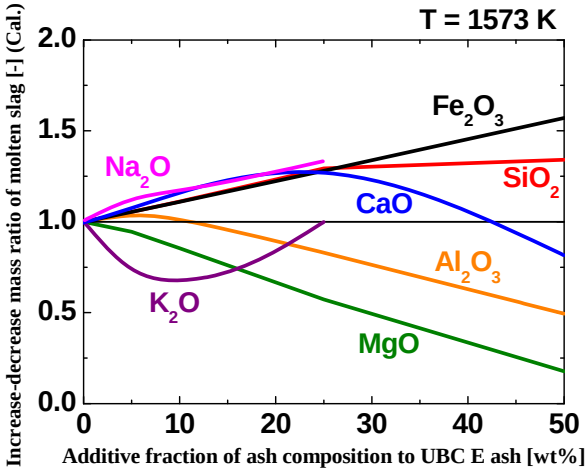

Figure 4. Relationship between additive fraction of each ash component in UBC E ash and the increase–decrease mass ratio of molten slag at 1573 K.

Figure 5 shows the relationship between the additive fraction of MgO and the molten slag fraction in the ash with MgO at 1573 K. From the figure, the molten slag fraction in UBC E ash indicated quite large values over 90%. The molten slag fraction in Coal A3 ash indicated a relatively low value around 40%. However, the molten slag fraction in ash with MgO decreased as the additive fraction of MgO in UBC E ash increased. As for UBC E ash, the molten slag fraction in ash with MgO became almost the same as that of Coal A3 ash when the additive fraction of MgO was 25%. Therefore, the MgO addition to UBC ash played a role in the decrease of the molten slag fraction in the ash.

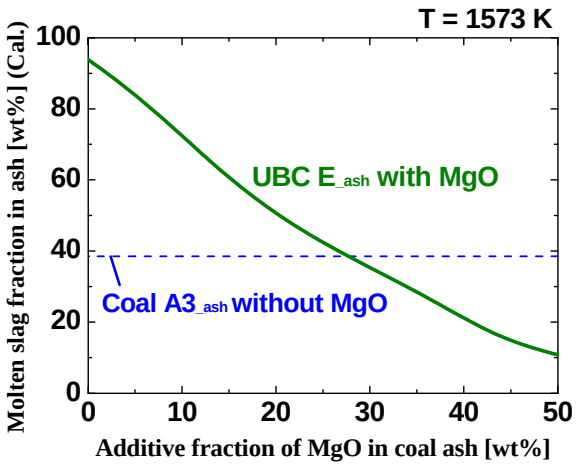

Figure 5. Relationship between additive fraction of MgO in coal ash and the molten slag fraction in the ash with MgO.

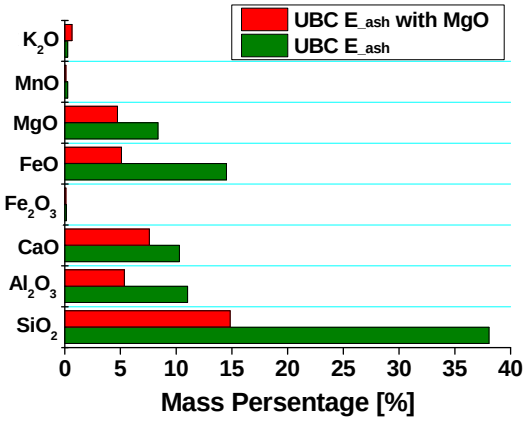

(a) Compositions in the molten slag phase.

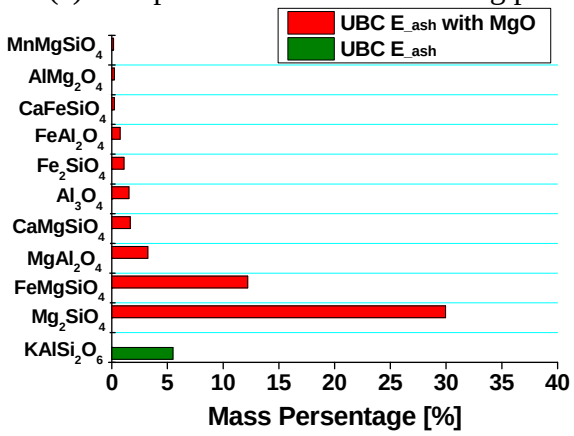

(b) Compositions in the solid phase.

Figure 6. Calculated results of the compositions in the molten slag and solid phases for UBC ash with and without MgO at 1573 K.

Figure 6 shows the calculated results of compositions in both the molten slag and solid phases for the UBC ash with and without MgO at 1573 K. The additive fraction of MgO is 25 wt% in the ash. The minor components with less than 0.1 wt% in both phases are negligible in this figure. For the UBC ash without MgO addition, SiO_2 slag was significant in the slag phase formed. When MgO was added, the fraction of the molten slag phase deceased, and some

alumino-silicates compounds were produced. As a result, a large amount of molten slag, including SiO_2 and FeO, decreased by adding MgO to the UBC ash.

5.2. Ash deposition behavior during coal combustion

Figure 7 shows photos of ash deposition on the tube for the UBC with and without MgO after 100 min of exposure time. For the UBC without MgO, most of the deposited ash was in a molten state. The deposition layer on the tube was very thin. For the UBC with MgO, on the other hand, the ash deposition layer was mainly composed of fine brown particles.

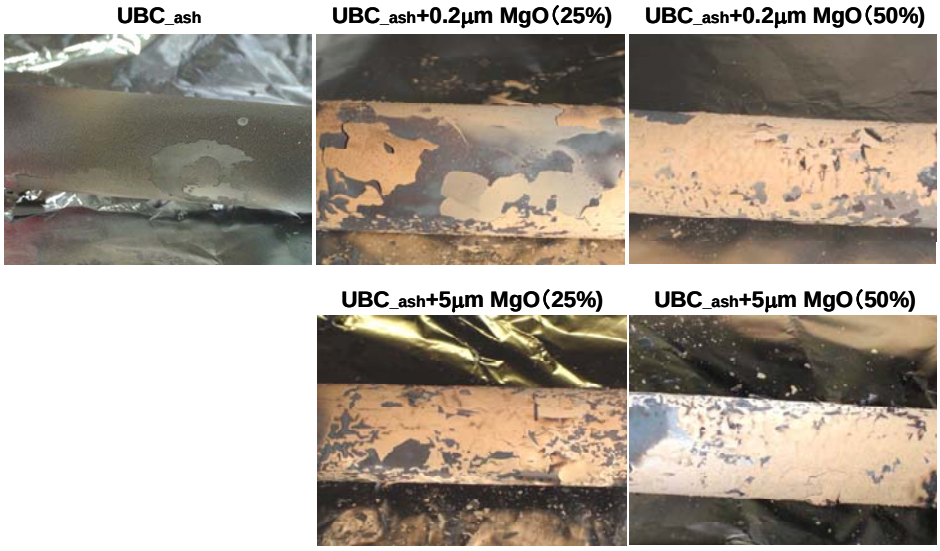

Figure 7. Photos of ash deposition on the tube after 100 min.

Figure 8 shows the relationship between the calculated molten slag fraction in the ash and the deposition fraction of ash (ϕ_{ash}) obtained experimentally. Here, ϕ_{ash} is defined as:

$$\phi_{ash} = \frac{D_{ash}}{F_{ash-probe} \cdot t} \tag{2}$$

$$F_{ash-probe} = \frac{A_p}{A_f} F_{ash-furnace} \tag{3}$$

In Eqs. (2) and (3), D_{ash} denotes the deposition mass of ash for a certain exposure time (t). $F_{ash\text{-}probe}$ and $F_{ash\text{-}furnace}$ are the mass flow rates of ash in the cross-sectional areas of the probe (A_p) and the furnace (A_f), respectively. The term $\phi_{ash\_t=100}$ is the experimental result after 100 min. As seen in the figure, the deposition fraction of ash also decreased with a decrease of the calculated molten slag fraction. This result suggested that MgO addition to the UBC E could contribute to reducing the ash deposition to the same level as that of Coal A3. Moreover, the smaller the particle diameter of MgO additive is, the more the rate of ash deposition lowers.

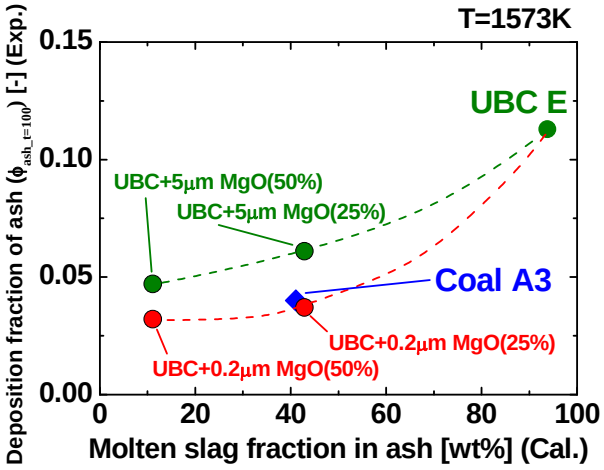

Figure 8. Relationship between molten slag fraction in the ash and the deposition fraction of the ash.

5.3. Mechanisms for the reduction of ash deposition

Figure 9 shows the cross-sectional structures and compositions of the ash particles just before adhering to the ash deposition tube. The additive fraction of MgO in the UBC ash was 25 wt%, and the mean particle diameter of added MgO was 0.2 μm. Comparing the Mg distributions for the UBC ash with and without MgO, for the UBC ash with MgO, Mg deposit on the surface of the ash particles.

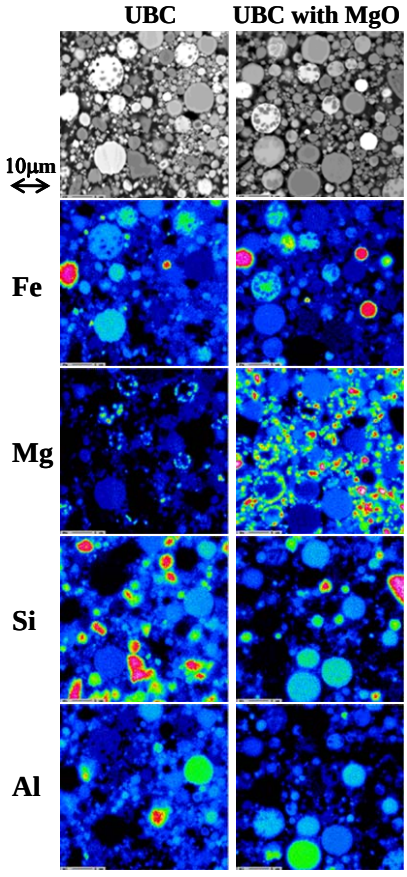

Figure 9. Cross-sectional structures and compositions of ash particles just before adhering to the ash deposition tube.

Figure 10 shows the cross-sectional structures and compositions of the deposit on the tube. We collected the samples of ash deposits on the tube after 10, 30, and 100 min of the exposure time. Comparing the results after 100 min for the UBC ash with and without MgO, a thick layer of Fe was produced for the UBC ash without MgO. This thick layer was mainly composed of Fe, Si, and Al. For the UBC ash with MgO, on the other hand, the layer was thinner, and Si and Al did not enrich the layer. As MgO was added to the UBC, the MgO concentration in the deposit increased. Based on these observations, Figure 11 summarizes the mechanisms for the reduction of the ash deposition for the UBC ash with MgO. For the UBC ash without MgO, the UBC ash directly reacted with the tube to produce an oxidized film that contained Fe, Si, and Al. For the UBC ash with MgO, on the contrary, the existence of MgO inhibited direct reactions between the ash particles and the tube surface. According to the results of the chemical equilibrium calculations mentioned above, MgO addition to the UBC could reduce the production of molten slag. In other words, the surface state of the deposit will always be dry so that the UBC ash with MgO did not easily adhere to the tube.

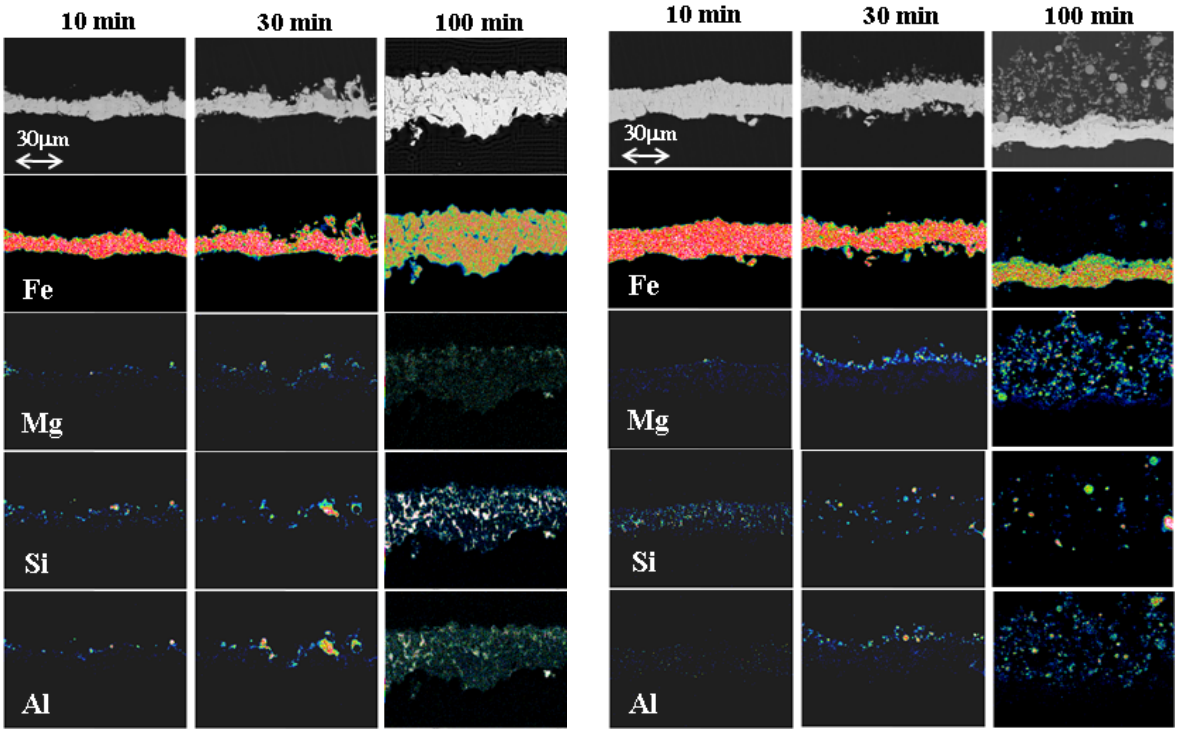

(a) UBC ash (b) UBC ash with MgO additive

Figure 10. Cross-sectional structures and compositions of the deposit on the tube.

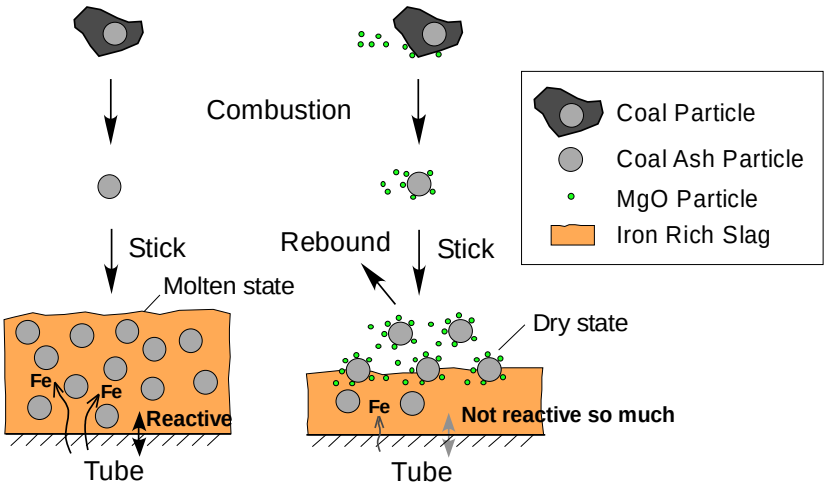

(a) UBC E (b) UBC E with MgO

Figure 11. Mechanisms for the reduction of ash deposition on the tube by MgO addition to the UBC.

6. Conclusions

We conducted chemical equilibrium calculations and ash deposition tests in order to evaluate the effects of MgO addition to the coal on the reduction of ash deposition for UBC and understand the reduction mechanisms of the ash deposition for the MgO addition. The MgO addition played a role in the decrease of the molten slag fraction. The amount of ash deposition for the UBC with MgO was relatively depressed. The MgO inhibited production of the molten slag on the tube. The smaller the particle diameter of MgO additive is, the more the rate of ash deposition lowers. One of the reduction mechanisms was due to the production of solid phase compositions of alumino-silicates due to MgO addition.

Acknowledgments

This study was partly supported by JCOAL, which provided our UBC sample.

References

[1] Sugita S, Deguchi T, Shigehisa T, Katsushima S. Demonstration of UBC Process in Indonesia, ICCS&T, Okinawa, Japan, Oct. 2005.

[2] Sugita S, Deguchi T, Shigehisa, T. Demonstration of a UBC (Upgrading of Brown Coal) Process in Indonesia. Kobe Steel Eng. Rep. 2006;56(2):23–26.

[3] Yamamoto S, Sugita S, Mito Y, Deguchi T, Shigehisa T, Otaka Y. Development of Upgraded Brown Coal Process, The Institute for Briquetting and Agglomeration (IBA), Savannah, GA, Oct. 2007.

[4] Akiyama, K, Tada, T. Combustion characteristics of upgraded brown coal (UBC), Proc. 6th Int. Symp. Coal Combust., China, 2007, 527–532.

[5] Frandsen, FJ. Ash Research from Palm Coast, Florida to Banff, Canada: Entry of Biomass in Modern Power Boilers. Energy Fuels 2009;23(7):3347–3378.

[6] Raask E. Mineral impurities in coal combustion, Hemisphere Publishing Corporation, Washington, 1985, 169–189.

[7] Walsh PM, Sayre AN, Loehden DO, Monroe LS, Beér JM, Sarofim AF. Deposition of bituminous coal ash on an isolated heat exchanger tube: Effects of coal properties on deposit growth. Prog. Energy Combust. Sci. 1990;16(4):327–345.

[8] Baxter LL. Influence of ash deposit chemistry and structure on physical and transport properties. Fuel Process. Technol. 1998;56 (1-2):81–88.
[9] Beer JM, Sarofim AF, Barta LE. Inorganic transformations and ash deposition during combustion. In Engineering Foundation; Benson, S. A., Ed, ASME: New York; 1992.
[10] Benson SA, Jones ML, Harb JN. Ash formation and deposition Chap.4. In Fundamentals of coal combustion for Clean and Efficient Use, Smoot, L. D., Ed, Elsevier Science, New York, 1993, p. 299.
[11] Naruse I, Kamihashira D, Khairil; Miyauchi Y, Kato Y, Yamashita T, Tominaga H. Fundamental ash deposition characteristics in pulverized coal reaction under high temperature conditions. Fuel 2005;84(4):405–410.
[12] Vuthaluru HB, Wall TF. Ash formation and deposition from a Victorian brown coal modelling and prevention. Fuel Process. Technol. 1998;53(3):215-233.
[13] Li S, Whitty K. J. Effect of Temperature and Residual Carbon. Energy Fuels 2009;23(4):1998–2005.
[14] Bai J, Li W, Li B. Characterization of low-temperature coal ash behaviors at high temperatures under reducing atmosphere. Fuel 2008;87(4-5):583–591.
[15] Abbott MF, Conn RE, Austin LG. Studies on slag deposit formation in pulverized-coal combustors: 5. Effect of flame temperature, thermal cycling of the steel substrate and time on the adhesion of slag drops to oxidized boiler steels. Fuel 1985;64(6):827–831.
[16] Harb JN, Munson CL, Richards,GH. Use of equilibrium calculations to predict the behavior of coal ash in combustion systems. Energy Fuels 1993;7(2):208–214.
[17] Hansen LA, Frandsen, FJ, Dam-Johansen K. Ash fusion quantification by means of thermal analysis, An Engineering Foundation Conference on Impact of Mineral Impurities in Solid Fuel Combustion, Hawaii, Nov., 1997.
[18] Ichikawa K, Oki Y, Inumaru J, Ashizawa M. Study on the Predicting Technique of Ash Deposition Tendency in the Entrained-Flow Coal Gasifier. Trans. Japan Soc. Mech. Eng., Ser. B 2001;67:144–150.
[19] Song, W. J, Tang, L. H, Zhu, X. D, Wu, Y. Q, Zhu, Z. B, Koyama, S. Effect of Coal Ash Composition on Ash Fusion Temperatures. Energy Fuels 2009;24(1):182–189.
[20] Akiyama K, Pak H, Tada T, Ueki Y, Yoshiie R, Naruse I. Ash Deposition Behavior of Upgraded Brown Coal and Bituminous Coal. Energy Fuels 2010; 24(8): 4138-4143.
[21] Pohl J.H, Creelman R.A, Ward C, Borio R, Radway G, Larsen G, Mehta A, Wolsiffer S, Davis C. Expanded Use of High-Surfur, Low-Fusion Coals in Utility Boilers: Effect of Additives. Proc. 26th Int. Tech. Conf. Coal Util. Fuel Syst. 2001, 597-608.
[22] Libutti B.L, Brandon J.H, Effective Use of Oxide Mixtures as Fuel Additives. Pap. NACE Conf. (Natl. Assoc. Corros. Eng.) 1975;162.
[23] Williams G.D, Cotton I.J. Energy and Maintenance Savings by Use of Fuel and Fireside Additive Programs. Proc. Refining Dep. Am. Pet. Inst. 1976;55, 819-839.
[24] Sinha R.K. High-Temperature Fireside Corrosion and Its Control by Chemical Additives. Mater Performance, 1992;31(4):44-49.
[25] FACT, www.crct.polymtl.ca
[26] C.W. Bale, P. Chartrand, S.A. Decterov, G. Eriksson, K. Hack, R. Ben Mahfoud, J. Melançon, A.D. Pelton and S. Petersen. FactSage Thermochemical Software and Databases. Calphad Journal, 2002;62, 189-228.